Feasibility of determining surface of matter density distributions of nuclei at RIBF

Akihisa Kohama,[*1] Ryoichi Seki,[*2,*3] Akito Arima,[*4] and Shuhei Yamaji[*1]

[*1] *RIBF Project Office, Cyclotron Center, RIKEN*

[*2] *Department of Physics and Astronomy, California State University, Northridge, USA*

[*3] *W. K. Kellogg Radiation Laboratory, California Institute of Technology, USA*

[*4] *The House of Councilors*

We show the feasibility of determining the surface of matter density distributions of nuclei from experimental data of low yields by demonstrating how the fitted density distributions lose their shapes with the quality of data in the framework of χ^2-fitting. We use various "pseudo data" for the fitting, which simulate upcoming experiments at the RI-Beam Factory of RIKEN. In doing so, we propose a new Gaussian basis function for the expansion of the density distribution, which is found to be convenient for numerical calculations. Our procedure is equally applicable to both stable and unstable nuclei, though we have unstable nuclei in mind.

Introduction

In the near future, the RI-Beam Factory (RIBF) of RIKEN will be able to provide lots of data on unstable nuclei.[1)] Their nature should be determined, particularly their sizes and their one-body matter density distributions, $\rho(\mathbf{r})$, because they are fundamental and important quantities for nuclear physics.[2, 3)] A consistent study of these quantities for unstable as well as stable nuclei will result in a deeper understanding of nuclear physics.[4)] It is high time that we should study the feasibility of determining them from upcoming experiments using the present plan of equipment.

To this end, we demonstrate how matter density distributions are affected by the quality of experimental data of the cross sections of proton-nucleus elastic scattering using a standard χ^2-fitting procedure. We use the word "quality of data" in the same meaning as the intensity of a nuclear beam. For example, when we say that the quality is low, we mean that the intensity is weak.

For the above demonstration, we use "pseudo data" which are created from random numbers distributed around theoretical cross sections calculated with a given density distribution at various momentum transfers. We take the case of p-^{58}Ni scattering as a test, and that of p-^{78}Ni scattering as a demonstration of unstable nuclei. We generate 25 sets of pseudo-data forming a pseudo-data-set group. A different pseudo-data-set group corresponds to a different intensity of the nuclear beam at the RIBF.

The density distribution, $\rho(\mathbf{r})$, is expanded in terms of some basis functions in order to avoid any assumption concerning the functional form of the density. The expansion coefficients are determined by minimizing χ^2 between the theoretical cross sections and the pseudo data. This is an application of the method of Friar and Negele.[5)] which was originally proposed to determine the charge distributions of stable nuclei from experimental data.

We use a new Gaussian basis function for the above expansion,[6)] the definition of which is given below. With the new Gaussian basis function, we can perform most of the integrals analytically, and the numerical calculations become much easier. Of course, we could use the popular Fourier-Bessel basis function by Friar and Negele.[5)] The Gaussian basis function of multiple center by Sick,[7)] or the delta-function basis function by Friedrich and Lenz [8)] are also candidates for the basis function of a χ^2-fitting. All of these four basis functions have the equal right to be the basis function of the fitting, and have different advantages.

In this note, we show that the surface region is determined from the experimental data of relatively low quality for the present plan of the RIBF. If we have a density distribution of monotonically decreasing function in r, such as the Woods-Saxon density, in mind, the surface is the region where $\rho(r)/\rho(0)$ varies from 0.9 to 0.1.[2)]

The full description of this work will appear elsewhere.[9)]

Formulation

Here, we explain our approach based on a χ^2-fitting in some detail. We apply the formulation of Friar and Negele.[5)]

We expand the one-body density distribution, $\rho(\mathbf{r})$, in M-terms of basis function, $\{f_n(\mathbf{r});\, n = 1, \cdots, M\}$ as

$$\rho(\mathbf{r}) \simeq \rho_M^{\rm fit}(\mathbf{r}) \equiv \sum_{n=1}^{M} C_n\, f_n(\mathbf{r}), \tag{1}$$

where $\rho_M^{\rm fit}(\mathbf{r})$ is the fitted density distribution. For simplicity, we assume the nuclei not to be deformed and examine only the radial dependence of the distribution. The fitted density distribution, Eq. (1), is then normalized to the mass number, A, as

$$\int d\mathbf{r}\, \rho_M^{\rm fit}(r) = 4\pi \int_0^\infty r^2 dr\, \rho_M^{\rm fit}(r) = A. \tag{2}$$

The expansion coefficients, C_n, are determined by minimizing χ^2 which is defined as

$$\chi^2(C_n) = \sum_{\alpha=1}^{N_{\rm data}} \frac{1}{\epsilon_\alpha^2} \left(\frac{d\sigma_\alpha^{\rm data}}{d\Omega} - \frac{d\sigma_\alpha^{\rm th}}{d\Omega}(C_n) \right)^2 . \quad (3)$$

Here, $d\sigma_\alpha/d\Omega$ is the differential cross section of proton-nucleus elastic scattering at θ_α, $N_{\rm data}$ is the number of data points, and ϵ_α is the uncertainty or error of each data point of θ_α. The superscript "data" of the cross section implies the experimental data, and "th" implies the value obtained theoretically. The subscript α specifies the order of the data point. The minimization of χ^2 is performed numerically using MINUIT in the CERN Library.

We use the expression of the first-order optical potential in the Glauber approximation,[10] the so-called eikonal expression, for the theoretical cross section in Eq. (3). This establishes the relation between the nuclear density that we wish to determine and the differential cross section from which we determine the density. While we consider (and also demonstrate later) the use of the approximated relation in terms of the eikonal expression appropriate to this model calculation at 1.047 GeV, it would be perhaps desirable to use a more rigorous relation based on the partial-wave decomposition and an improved optical potential for lower energies, because various experiments at the RIBF are expected to be carried out at around 500 MeV or even lower energies. In our model calculation, we assume the relation to be exact and generate pseudo data using it, because no real, experimental datum of differential cross section enters our analysis at all. Since we wish to draw a conclusion relevant to future experiments, the relation should be reasonably accurate and also the density that we use should be also reasonably realistic.

As the basis functions of Eq. (1), we use Gaussian basis functions with a cutoff at R:

$$f_n(r) = \exp(-r^2/r_n^2)\ \theta(R-r), \quad (n = 1, \cdots, M), \quad (4)$$

where r_n is the size parameter defined in the geometrical progression, $r_n = r_1 a^{n-1}$ $(n = 1, \cdots, M)$.[6] These Gaussian basis functions differ from those used previously by Sick, [7] and will be referred to as "Kamimura-Gauss (KG) basis functions" after the author who has used them extensively.

Pseudo data

We create a total of 25 sets of pseudo data. Each pseudo-data set (PD set) mimics experimental data obtained by a series of measurements, and consists of the proton-nucleus elastic scattering cross sections at the center-of-mass scattering angles that are common to all PD sets. An uncertainty is assigned to each cross section.

At each scattering angle, θ_α, we generate 25 cross sections. They are generated artificially, but in a way as realistic as possible. The following steps are taken to this end. First, we calculate the "theoretical" cross section $d\sigma_\alpha^{\rm th}/d\Omega$ from the given nuclear density of a three-parameter Fermi distribution form. Second, 25 cross sections are generated, randomly distributed about the "theoretical" cross section. Third, an uncertainty is assigned to each datum generated.

Let us elaborate on these steps. In the second step, 25 cross sections are generated following the Gaussian distribution,

$$f(x;\mu,\sigma^2) = \frac{1}{\sqrt{2\pi\sigma^2}}\ \exp\{\frac{-(x-\mu)^2}{2\sigma^2}\}, \quad (5)$$

where μ is the mean and σ is the standard deviation which we specify as $\mu = d\sigma_\alpha^{\rm th}/d\Omega$ and $\sigma = \mu/\sqrt{N_{\rm yield}(\theta_\alpha)}$, respectively. Here, we define the yield count,

$$N_{\rm yield}(\theta_\alpha) = \frac{N_0}{B_0}\ \frac{d\sigma_\alpha^{\rm th}}{d\Omega}, \quad (6)$$

where B_0/N_0 [mb/str] is the measurement efficiency, the magnitude of the cross section that yields a unit count in the measurement.

We set $N_0 = 10$ so that $\sigma = 0.316\mu$ when $d\sigma_\alpha^{\rm th}/d\Omega = B_0$, and examine three cases of $B_0 = 0.1$, 1.0, and 10.0 mb/str. Note that the data less than B_0/N_0 is rejected, because $N_{\rm yield}(\theta_\alpha)$ of Eq. (6) becomes less than one.

In the third step, we assign an uncertainty to each pseudo datum, using the same expression of σ below Eq. (5), except for $d\sigma_\alpha^{\rm th}/d\Omega$ of Eq. (6) being replaced by the pseudo datum itself, $d\sigma_\alpha^{\rm PD}/d\Omega$.

The center-of-mass scattering angle is taken to be greater than 4°, based on the expected experimental setups (in inverse kinematics) at the RIBF. The set of angles, $\{\theta_\alpha\}$, is chosen with 1.0° separation ($\Delta\theta_0 = 1.0°$), but the separation is reduced near the forward direction if the statistical uncertainty becomes less than $\epsilon_{\rm min}$.[9] The number of data in each PD set, $N_{\rm data}$, is then made to be more than 20, which provides the number of degrees of freedom, $N_{\rm dof}$ ($\equiv N_{\rm data} - M$), suitable for the least-square fitting procedure that we will carry out for $M = 10$.

By picking up one of the pseudo data at each θ_α, we can make 25 PD sets. The i-th PD set consists of $\{d\sigma_\alpha^{{\rm PD},i}/d\Omega;$ $\alpha = 1, \cdots, N_{\rm data}\}$. A PD set corresponds to a series of measurements to obtain an angular distribution. The 25 PD sets form a PD-set group that corresponds to 25 series of measurements.

Following the above steps, we create three kinds of PD-set groups classified by B_0 [mb/str]. We take $B_0 = 0.1$ mb/str for PD-set group A, $B_0 = 1.0$ mb/str for PD-set group B, and $B_0 = 10.0$ mb/str for PD-set group C. We take $\epsilon_{\rm min} = 2.0$, 3.3, and 6.7% for PD-set groups A, B, and C, respectively (Table 1).

The kinematical conditions are: $\theta_{\rm max} \leq 25° \Leftrightarrow q_{\rm max} \leq 750$ MeV, and $\Delta\theta \simeq 1.0° \Leftrightarrow \Delta q \simeq 20$ MeV, where Δq is an increment in momentum transfer. Since we take a step in θ smaller than 1° in the forward direction, Δq can be made

Table 1. Parameters of pseudo-data-set group A, B, and C, respectively. B_0 is the magnitude of cross section corresponding to yield N_0. $N_0 = 10$ in this work. $\epsilon_{\rm min}$ [%] is the minimum uncertainty. $\Delta\theta_{\rm min}$ [mrad] is the minimum step.

Group	B_0 [mb/str]	$\epsilon_{\rm min}$ [%]	$\Delta\theta_{\rm min}$ [mrad]	Rate [s^{-1}]
A	0.1	2.0	2×0.3	10^3
B	1.0	3.3	2×0.3	10^2
C	10.0	6.7	2×0.3	10

smaller. Some of the parameters for the expansion of the density distribution are related to the kinematical conditions of the experiment.[5] The following are the rough estimates of them: $r_{\max}$ is the maximum probing distance in the experiment, and $r_{\max} \simeq \pi/\Delta q \simeq 30\,\mathrm{fm}$. We take $R = 10\,\mathrm{fm}$ ($\leq r_{\max}$). The resolution of the fitted density distribution is $\Delta r = \pi/q_{\max} \simeq 0.85\,\mathrm{fm}$. The dimension of the model space is $M \simeq q_{\max} R/\pi$. We estimate $M \simeq 10$–15, and will conduct numerical calculations for $M = 10$ in the following.

After the estimations based on the setups of the RIBF are made, we find that the line of 0.1 mb/str roughly corresponds to 10 yield counts for the above conditions, which is PD-set group A.[9] The correspondence of the rate of particle production to the PD-set group is also summarized in Table 1. As far as nickel isotopes are concerned, ^{70}Ni is produced at a rate of about $10^3\,\mathrm{s}^{-1}$, which corresponds to PD-set group A for the present plan of RIBF. ^{78}Ni corresponds to PD-set group C, because the production rate is about $10\,\mathrm{s}^{-1}$.

χ^2-fitting

With those pseudo-data-set (PD-set) groups of p-^{58}Ni elastic scattering created in the previous subsection, we make χ^2-fittings, Eq. (3), to obtain the density distributions, $\rho(r)$, using the KG basis function, $f_n(r)$, of Eq. (4). In doing the fittings, we treat the normalization of $\rho(r)$ as a datum with very small uncertainty, such as 58.0±0.1 for ^{58}Ni.

The numerical results for PD-set groups A, B, and C are shown in Figs. 1, 2, and 3, respectively, with $R = 10\,\mathrm{fm}$ and $M = 10$. The rate of particle production decreases from PD-set group A to group C (see Table 1), and the quality of the pseudo data becomes worse in this order.

In a) of those figures, we plot 25 fitted cross sections (solid curve) and all the pseudo data (cross with bar). The dips of the fitted cross sections appear very sharp, because we neglect the Coulomb interaction for simplicity, which is known to fill each dip.[11,12] Our theoretical curve with the three-parameter Fermi density distribution is consistent with the experimental data of SATURN, Saclay,[13] except for the depth of each dip. The average values of χ^2 divided by the number of degrees of freedom (DOF), χ^2/DOF, obtained from the 25 different PD sets are also shown. For every case, χ^2/DOF is about one, and the variance increases from PD-set group A to group C, reflecting the quality of pseudo-data.

In b) of those figures, we plot 25 fitted density distributions, (solid curve), and the original density distribution (dotted curve) in the form of $r^2 \times \rho_M^{\mathrm{fit}}(r)$, because it is this form that

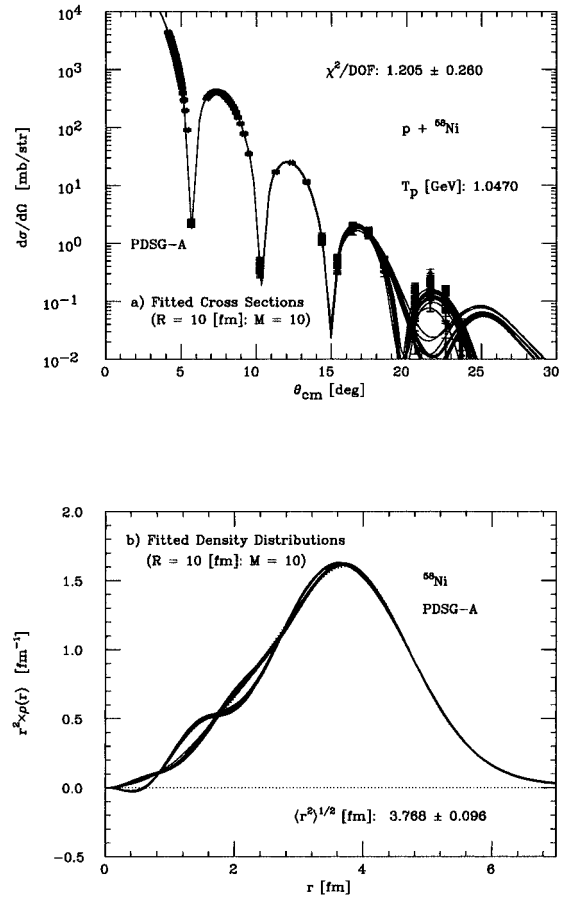

Fig. 1. Results of χ^2-fitting for the pseudo-data set group (PDSG)-A of ^{58}Ni. $R = 10\,\mathrm{fm}$ and $M = 10$. a) 25 fitted cross sections (solid curve) and all the pseudo data (cross with bar). b) 25 fitted density distributions (solid curve), and the original distribution (dotted curve). The density distributions are drawn in the form of $r^2\,\rho(r)$.

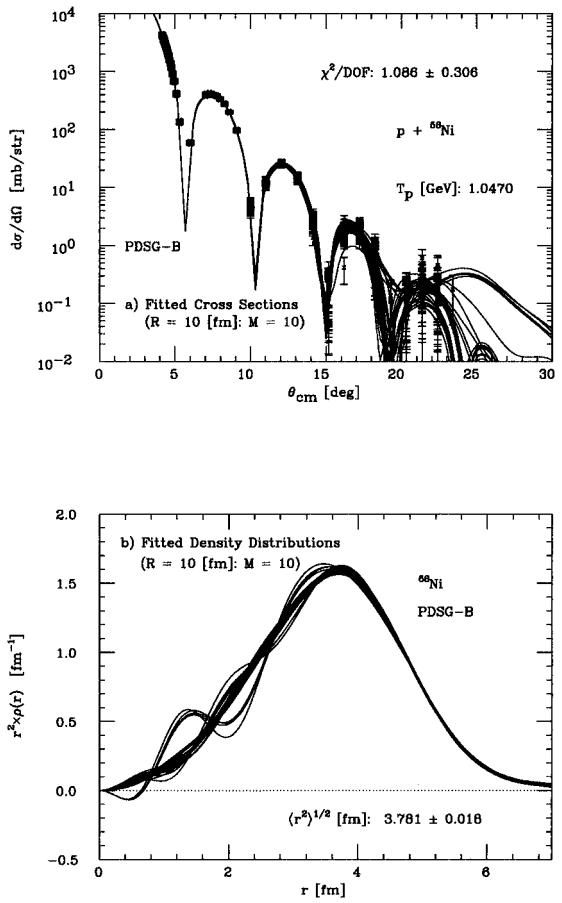

Fig. 2. Results of χ^2-fitting for the pseudo-data set group (PDSG)-B of ^{58}Ni. $R = 10\,\mathrm{fm}$ and $M = 10$. a) and b) are the same as Fig. 1.

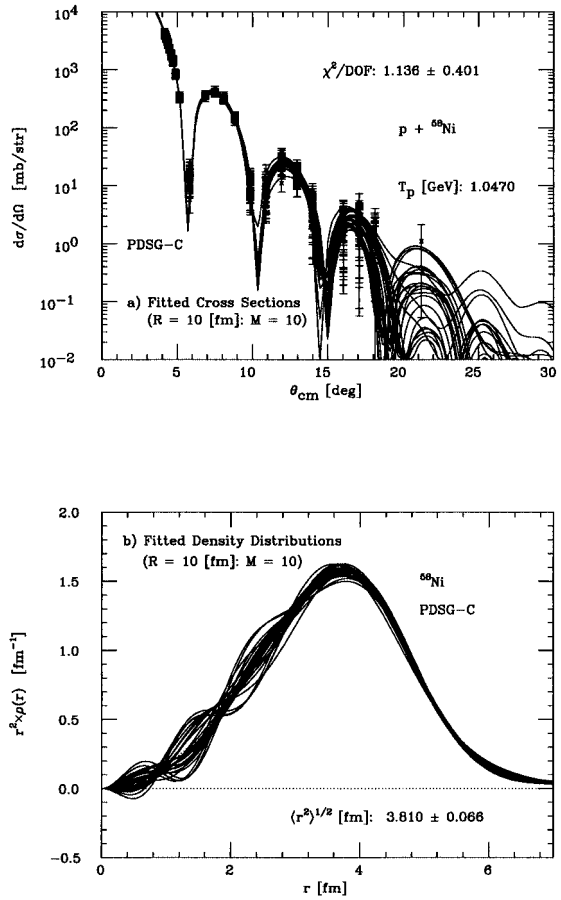

Fig. 3. Results of χ^2-fitting for the pseudo-data set group (PDSG)-C of ^{58}Ni. $R = 10$ fm and $M = 10$. a) and b) are the same as Fig. 1.

the normalization integral constrains. Although the density distributions are multiplied by r^2, they still have large uncertainties in the central region while they have small uncertainties in the surface for all the PD-set groups, which is a situation similar to that of the charge density distribution. The original distribution drawn by the dotted curve is included in the band of 25 fitted densities, which signifies that our procedure consistently provides probable density distributions within the uncertainty. The RMS radius, $\langle r^2 \rangle^{1/2}$, obtained from the 25 different PD sets is also shown. Each of them has less than 2% uncertainty, and the original value, $\langle r^2 \rangle^{1/2} = 3.764$ fm is included in the uncertainty. Even with PD-set groups of lower yields, it appears that the surface has smaller uncertainty than the center. It is reasonable that the surface region of $\rho_M^{\rm fit}(r)$ is determined, because the cross section carries the information of this region.[13)]

Some of the fitted cross sections of Fig. 1 a) have different dip positions from those of the pseudo data for $\theta_{\rm cm} > 20^\circ$, while the dip positions of the fitted cross sections are quite close to those of the pseudo data for PD-set groups B and C. Even though some of the fitted cross sections do not reproduce the pseudo data in $\theta_{\rm cm} > 20^\circ$ in Fig. 1 a), the fitted density distributions do not fluctuate largely in Fig. 1 b). This suggests that the pseudo data with an uncertainty of 30% in this region of θ weakly affect the density distribution. If we increase the number of terms of the KG basis, M, to 15, this behavior disappears, and χ^2/DOF improves, but the fluctuations in the fitted density distributions increase. The above occurs, because $M = 10$ is a bit small to fit the large number of the pseudo data like PD-set group A.[5)] The best choice of M would be 10–15 for PD-set group A. We only show the cases of $M = 10$ for the discussion of the statistical and the systematic errors below.

Error estimations

When the true value, $X_{\rm true}$, is known, the mean square error of a measured value, $X_{\rm data}$, is defined as[14)]

$$\langle (X_{\rm data} - X_{\rm true})^2 \rangle = \langle (X_{\rm data} - \langle X_{\rm data} \rangle)^2 \rangle + (\langle X_{\rm data} \rangle - X_{\rm true})^2, \quad (7)$$

$$\equiv \sigma^2 + b^2, \quad (8)$$

where the bracket, $\langle A \rangle$, implies the sample mean of A. σ is the statistical error, and b is the systematic error or the bias. Generally, the error contained in data is an independent sum of the statistical and systematic errors. The statistical error shows how large the fitted results fluctuate around the sample mean, while the systematic error shows the deviation of the sample means from the true value.[14)]

By applying the above relation, we can define the statistical and systematic errors for the fitted density distributions as

$$\sigma_\rho(r)^2 \equiv \langle \left(\rho_M^{\rm fit}(r) - \langle \rho_M^{\rm fit}(r) \rangle \right)^2 \rangle, \quad (9)$$

$$b_\rho(r)^2 \equiv \left(\langle \rho_M^{\rm fit}(r) \rangle - \rho_{\rm true}(r) \right)^2, \quad (10)$$

where the sample mean is defined by

$$\langle \rho_M^{\rm fit}(r) \rangle \equiv \frac{1}{n} \sum_{i=1}^{n} \rho_M^{{\rm fit},i}(r), \quad (11)$$

where n is the number of PD sets, $n = 25$.

In order to see whether one can determine the density distributions in the surface region, we show the numerical results of the statistical and systematic errors, defined above. The statistical errors for the fitted density distributions, $\sigma_\rho(r)$, Eq. (9), are shown in Fig. 4 a), and the systematic errors, $b_\rho(r)$, Eq. (10), in Fig. 4 b). They are divided by $\rho_{\rm true}(r)$ to clarify the relative magnitude. From Fig. 4 a), one can see that the statistical errors precisely reflect the quality of PD-set group, particularly in the surface region, $r = 2$–6 fm, and have large uncertainties in the central region. The uncertainty increases as the quality of the pseudo data becomes worse. From Fig. 4 b), one can see that the systematic errors scarcely depend on the PD-set groups. The systematic errors behave similarly to the completeness errors, although the magnitude is one order larger.

From those observations, we confirm that the surface is really determined by those PD-set groups, because the statistical and systematic errors for the fitted density distributions are both small in the surface region. Even with PD-set group of lower yield, it appears that the surface has smaller uncertainty than the center.

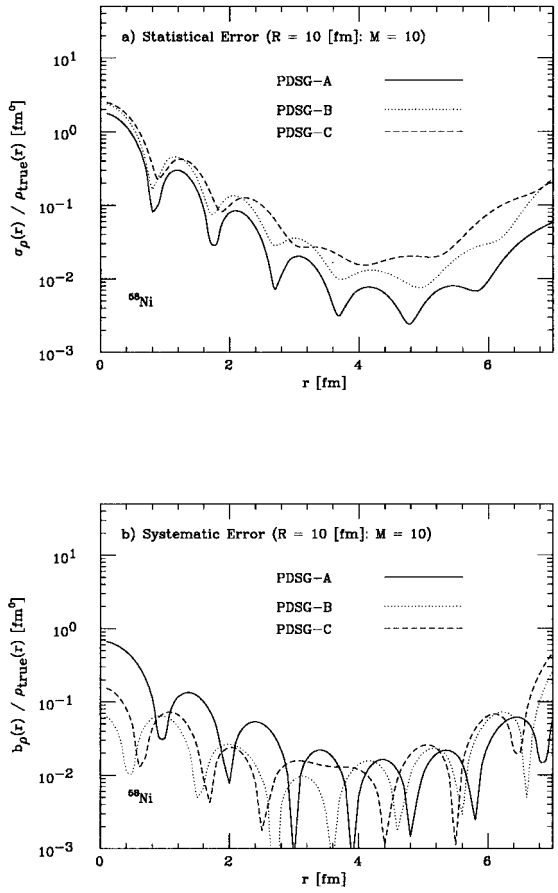

Fig. 4. a) Statistical error, and b) systematic error of the fitted density distributions for ^{58}Ni. We divide them by $\rho_{\rm true}(r)$ at each r. The solid curve is the case of PD-set group A, the dotted curve is the case of PD-set group B, the dashed curve is the case of PD-set group C.

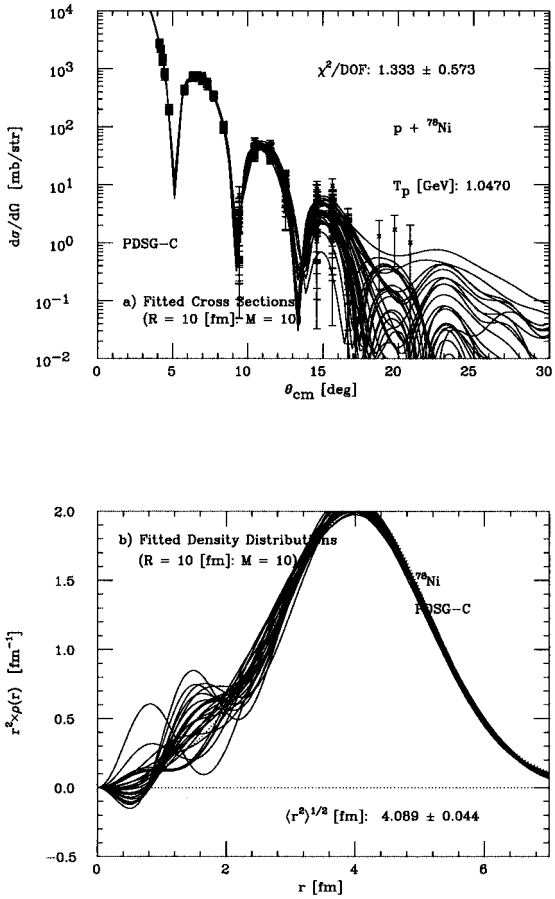

Fig. 5. Results of χ^2-fitting for the pseudo-data set group (PDSG)-C of ^{78}Ni. $R = 10\,$fm and $M = 10$. a) and b) are the same as Fig. 1.

Application

As an application in our framework, we make χ^2-fittings with the pseudo data of p-^{78}Ni elastic scattering. We apply the condition for PD-set group C to create the pseudo data, because the rate of particle production of ^{78}Ni at the RIBF is $10\,\mathrm{s}^{-1}$. As an example, we use the vector part of the densities obtained in the relativistic mean field theory for the density distribution to create the pseudo data.

The numerical results of χ^2-fittings are shown in Figs. 5 a) and b). We use $R = 10\,$fm and $M = 10$. The size parameters, $r_1 = 1.0\,$fm, and $r_M = 5.5\,$fm, have the same values as those of ^{58}Ni. The pseudo data are fitted well, especially in the forward direction, in Fig. 5 a). As one can see from Fig. 5 b), the fitted density distributions fluctuate in the central region, but are stable in the surface region where the bump structure exists in the original density distribution. We have a good chance to determine such distribution of unstable nuclei. The RMS radius obtained from the fittings is slightly smaller than the original one, $\langle r^2\rangle^{1/2} = 4.181\,$fm. The behavior of the systematic and statistical uncertainties is almost similar to those obtained for the case of ^{58}Ni (Fig. 6). Thus, it is possible to better determine the surface region of ^{78}Ni than the central region, and probably of unstable nuclei.

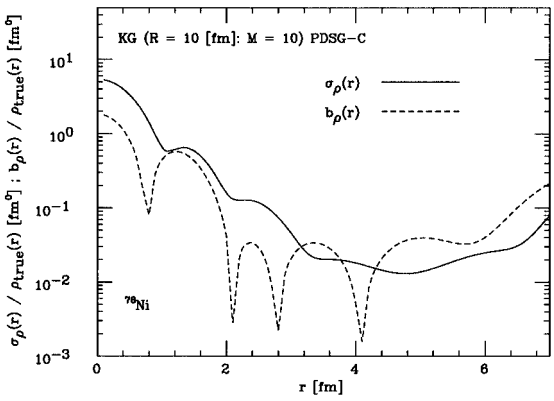

Fig. 6. Statistical error and systematic error of the fitted density distributions for ^{78}Ni. The solid curve is the statistical error and the dashed curve is the systematic error. They are divided by $\rho_{\rm true}(r)$.

Summary and conclusion

We have shown the feasibility to determine the surface of matter density distribution of nuclei from experimental data, and conclude that the surface extension of the density distribution can be determined well even if the intensity of the

nuclear beam is relatively low, namely, of the order of $10\,\mathrm{s}^{-1}$, for the present setup of the RIBF of RIKEN. This intensity corresponds to ^{78}Ni. We have used three kinds of pseudo-data set groups of the cross section of proton-nucleus elastic scattering, each of which corresponds to a different nuclear beam intensity. This simulates upcoming experiments at the RIBF. The statistical errors are found to concentrate at the central region of $\rho_M^{\mathrm{fit}}(r)$, which is a situation similar to that of the charge density distribution. The central region of the fitted density distributions loses its shape as the quality of data becomes worse.

The density distribution, $\rho(r)$, is expanded in terms of the KG basis function in order to avoid any assumption on the functional form of the density. We have firstly applied this basis function to the analysis of the density distribution of nuclei. We have shown that the KG basis function has the same right to be the basis function for such analysis by χ^2-fitting as the basis functions proposed before. Once we determine the size parameters for each M to a known density distribution, such as the Woods-Saxon distribution for stable nuclei, we can fit those of the isotopes with the same parameters as we have illustrated with the example of ^{78}Ni. We believe that our results have weak dependence on the choice of the basis function, and will report the confirmation of this issue in our future work.

We acknowledge I. Tanihata for his invaluable suggestions and comments, and M. Kamimura and K. Yazaki for stimulating discussions. We thank T. Ohnishi, and T. Suda, and K. Katori for helping us generate pseudo data by clarifying the expected experimental setups at the RIBF. G. D. Alkhazov and A. Lobodenko informed us of their work.[12)] This work is supported under the Special Postdoctoral Research Program at RIKEN and by the U.S. DOE at CSUN (DE-FG03-87ER40347) and the U.S. NSF at Caltech (PHY-9722428 and PHY-9420470).

References

1) Y. Yano, T. Katayama, A. Goto, and M. Kase: AIP Proc. 16th Int. Conf. on the Application of Accelerators in Research and Industry, Denton, Texas, USA, 2000-11, to be published.
2) L. R. B. Elton: *Nuclear Sizes* (Oxford University Press, Oxford, 1961).
3) A. Chaumeaux et al.: Ann. Phys. (NY) **116**, 247 (1978).
4) I. Tanihata et al.: Phys. Lett. B **160**, 380 (1985).
5) J. L. Friar and J. W. Negele: Adv. Nucl. Phys. **8**, 219 (1975).
6) M. Kamimura: Phys. Rev. A **38**, 621 (1988).
7) I. Sick: Nucl. Phys. A **218**, 509 (1974).
8) J. Friedrich and F. Lenz: Nucl. Phys. A **183**, 523 (1972).
9) A. Kohama, R. Seki, A. Arima, and S. Yamaji: in preparation.
10) R. J. Glauber: in *Lectures in Theoretical Physics*, Vol. 1, edited by W. E. Brittin and D. G. Dunham (Interscience, New York, 1959) p. 315.
11) W. Czyz, L. Leśniak, and H. Wolek: Nucl. Phys. B **19**, 125 (1970).
12) R. D. Amado, J. P. Dedonder, and F. Lenz: Phys. Rev. C **21**, 647 (1980).
13) R. M. Lombard et al.: Nucl. Phys. A **360**, 233 (1981).
14) G. Cowan: *Statistical Data Analysis* (Clarendon Press, Oxford, 1998).